Biochemical mechanism of action of a diketopiperazine inactivator of plasminogen activator inhibitor-1

Anja P. EINHOLM*[1], Katrine E. PEDERSEN*[1], Troels WIND*, Paulina KULIG*, Michael T. OVERGAARD*, Jan K. JENSEN*, Julie S. BØDKER*, Anni CHRISTENSEN*, Peter CHARLTON† and Peter A. ANDREASEN*[2]

*Department of Molecular Biology, Aarhus University, 10C Gustav Wied's Vej, 8000 C Aarhus, Denmark, and †Xenova, 957 Buckingham Avenue, Slough, Berkshire, SL1 4NL, U.K.

XR5118 [(3*Z*,6*Z*)-6-benzylidine-3-(5-(2-dimethylaminoethyl-thio-))-2-(thienyl)methylene-2,5-dipiperazinedione hydrochloride] can inactivate the anti-proteolytic activity of the serpin plasminogen activator inhibitor-1 (PAI-1), a potential therapeutic target in cancer and cardiovascular diseases. Serpins inhibit their target proteases by the P_1 residue of their reactive centre loop (RCL) forming an ester bond with the active-site serine residue of the protease, followed by insertion of the RCL into the serpin's large central β-sheet A. In the present study, we show that the RCL of XR5118-inactivated PAI-1 is inert to reaction with its target proteases and has a decreased susceptibility to non-target proteases, in spite of a generally increased proteolytic susceptibility of specific peptide bonds elsewhere in PAI-1. The properties of XR5118-inactivated PAI-1 were different from those of the so-called latent form of PAI-1. Alanine substitution of several individual residues decreased the susceptibility of PAI-1 to XR5118. The localization of these residues in the three-dimensional structure of PAI-1 suggested that the XR5118-induced inactivating conformational change requires mobility of α-helix F, situated above β-sheet A, and is in agreement with the hypothesis that XR5118 binds laterally to β-sheet A. These results improve our understanding of the unique conformational flexibility of serpins and the biochemical basis for using PAI-1 as a therapeutic target.

Key words: cancer, protease, serpin, therapeutic target, thrombosis.

INTRODUCTION

The tissue- and urokinase-type plasminogen activators (tPA and uPA respectively) are serine proteases catalysing proteolytic conversion of the zymogen plasminogen into the active serine protease plasmin. Plasmin can degrade fibrin and other extracellular proteins. The activities of tPA and uPA are regulated by plasminogen activator inhibitor-1 (PAI-1; see [1] for a review). The relative plasma levels of tPA and PAI-1 regulate the fibrinolytic capacity of blood (see [2] for a review). In human beings, an increased plasma PAI-1 level is associated with an increased risk of thrombotic disease (see [3] for a review). Transgenic mice with an increased plasma PAI-1 level develop thrombosis [4,5]. Moreover, plasminogen activation is also suggested to play a role in the spread of cancers, by uPA-catalysed plasmin generation in tumours, leading to degradation of basement membranes, thereby enabling the cancer cells to invade normal tissue. This idea has been supported by evidence from various model systems and by the observation that a high tumour level of uPA is correlated with a poor prognosis (see [1,6] for reviews). It was therefore surprising initially that a high tumour level of PAI-1 is an even better marker for a poor prognosis (see [1,6] for reviews). The function of PAI-1 in the spread of malignant tumours is not known completely, but one important aspect seems to be a proangiogenic effect of PAI-1 [7–11]. Inactivation of PAI-1 is therefore of potential therapeutic value in thrombotic and in cancerous diseases.

PAI-1 belongs to the serpin protein family. The distinguishing biochemical feature of serpins is their ability to undergo a characteristic change from a metastable, so-called stressed (S) conformation to a more stable, so-called relaxed (R) conformation, consisting of the insertion of the surface-exposed reactive centre loop (RCL) as strand 4 of the central β-sheet A (s4A; Figure 1; see [12,13] for reviews). During the reaction of a serpin with its target protease, the P_1–P_1' bond in the RCL is cleaved by the protease, which thereby becomes attached to the P_1 residue of the serpin by an ester bond to the protease active-site serine residue. Subsequently, the protease is translocated to the opposite pole of the serpin. The protease is thereby distorted and is not able to catalyse hydrolysis of the ester bond, resulting in a stable serpin–protease complex [14–22]. In some situations, RCL insertion cannot keep pace with ester bond hydrolysis, resulting in P_1–P_1' bond cleavage and serpin substrate behaviour (see [13] for a review). For some serpins, including PAI-1, the RCL can insert into β-sheet A without P_1–P_1' bond cleavage, resulting in the formation of a relaxed, so-called 'latent state' [23]. During RCL insertion, there are also conformational changes in the so-called flexible joint regions of serpins around α-helix (h) D and E. In PAI-1, a hydrophobic cavity in this region is rearranged at the RCL insertion (Figure 1 and [24–26]).

There are several ways of blocking the serpin-inhibitory mechanism, such as conversion of the serpin into an inactive form before the encounter with the protease, inhibition of the initial encounter between protease and serpin and inhibition of the serpin conformational changes associated with complex formation. A variety of amphipathic organochemical neutralizers of PAI-1 have been identified previously [26–31]. We have shown

Abbreviations used: bis-ANS, 4,4′-dianilino-1,1′-bisnaphthyl-5,5′-disulphonic acid, dipotassium salt; h, α-helix; HBS, Hepes-buffered saline; HMK, heart muscle kinase; PAI-1, plasminogen activator inhibitor-1; s, strand in a β-sheet; s4A, strand 4 of the central β-sheet A; RCL, reactive centre loop; tPA, tissue-type plasminogen activator; TUG, transverse urea gradient; uPA, urokinase-type plasminogen activator; XR5118, (3*Z*,6*Z*)-6-benzylidine-3-(5-(2-dimethylaminoethyl-thio-))-2-(thienyl)methylene-2,5-dipiperazinedione hydrochloride; for brevity the one-letter system for amino acids has been used, V345, for example, means Val^{345}.

[1] These authors have contributed equally to this work.

[2] To whom correspondence should be addressed (e-mail pa@mb.au.dk).

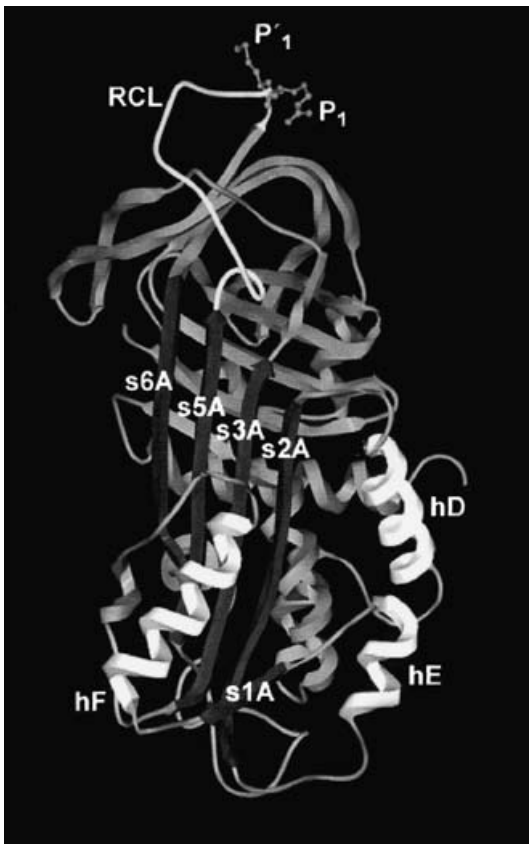

Figure 1 Three-dimensional structure of PAI-1

Ribbon presentation of the three-dimensional structure of PAI-1 in the active form. The RCL and α-helices (**D**–**F**) are shown in white and β-sheet A in dark grey. P_1–P_1' residues are indicated by ball and stick. The Figure is a Swiss-PDB-Viewer display of the X-ray crystal structure as determined by Sharp et al. [24].

previously that a group of negatively charged amphipathic compounds inactivates PAI-1 by converting it into polymers, whereas PAI-1 inactivated by the positively charged XR5118 [(3*Z*,6*Z*)-6-benzylidine-3-(5-(2-dimethylamonoethyl-thio-))-2-(thienyl)methylene-2,5-dipiperazinedione hydrochloride] is in a monomeric form [26]. We have now characterized further the XR5118-induced inactive PAI-1 form.

EXPERIMENTAL

Cloning, mutagenesis and purification of PAI-1

The cDNA for human PAI-1 was modified to include an N-terminal His_6 tag and a recognition motif for heart muscle kinase (HMK) and cloned into the *Escherichia coli* expression vector pT7-P [32]. Mutations in PAI-1 were introduced using the QuickChange Site-Directed Mutagenesis kit (Stratagene, La Jolla, CA, U.S.A.) following the manufacturer's instructions, except that the final product was electroporated into *E. coli* DH5α cells, and confirmed by sequencing using the Thermo Sequenase II Dye Terminator Cycle Sequencing kit (Amersham Biosciences, Uppsala, Sweden) and a 373A ABI sequencer (Applied Biosystems, Foster City, CA, U.S.A.).

PAI-1 protein was expressed in *E. coli* BL21(DE3)pLysS cells (Novagen, Madison, WI, U.S.A.) and purified from homogenized bacteria by an Ni^{2+}-nitrilotriacetate column (Qiagen, Albertslund, Denmark) and gel-filtration on a Superdex 75 column (1.6 cm × 60 cm; Amersham Biosciences). Concentration of the purified PAI-1 was determined from the absorbance A_{280} value using the calculated molar absorption coefficient 34650 litre · mol^{-1} · cm^{-1} [33]. It was stored at −80 °C in Hepes-buffered saline [HBS: 10 mM Hepes (pH 7.4)/0.14 M NaCl], supplemented with 5 % (w/v) glycerol and NaCl to a final concentration of 1 M. This procedure gave 2–15 mg of PAI-1 per litre of culture routinely. N-terminal sequencing revealed that the recombinant protein had the expected N-terminus, i.e. (M)GSMGSHHHHHHGS-RRASV3 . . . , where the initiating methionine residue in parentheses was missing and the order of the original PAI-1 residues serine (S) and alanine (A) were changed. Reactivity of PAI-1 in terms of uPA inhibition and vitronectin binding was not affected by the His_6 and HMK tags [34]. The HMK site (underlined) allows labelling of the molecule with ^{32}P [35].

Active PAI-1 was converted into the latent state by 24 h incubation in HBS at 37 °C. P_1–P_1' bond cleaved PAI-1 was produced as described previously [36].

Numbering of PAI-1 residues was S1-A2-V3-H4-H5 . . . [37]. The N-terminal extension was numbered G(−15)-S(−14)-S(−13) . . . .

Miscellaneous proteins and materials

XR5118 was synthesized as described previously [28]. Stock solutions with millimolar concentrations of XR5118 were prepared in 5 % (w/v) DMSO and 0.15 % lactic acid (referred to as XR5118 vehicle). The following materials were purchased from the indicated sources: bis-ANS (4,4′-dianilino-1,1′-bisnaphthyl-5,5′-disulphonic acid, dipotassium salt; Molecular Probes, Eugene, OR, U.S.A.); elastase, endoprotease Glu-C, endoprotease Lys-C and papain (Roche Applied Bioscience, Mannheim, Germany); pig gelatin (Sigma); pyroEGR-*p*-nitroanilide (S-2444; Chromogenix, Mölndal, Sweden); subtilisin (Sigma); polymeric vitronectin (Becton Dickinson, Bedford, MA, U.S.A.); and human uPA (Wakamoto Pharmaceutical Co., Tokyo, Japan).

SDS/PAGE

SDS/PAGE was performed either on gels with 11 % (w/v) polyacrylamide or by the Tricine–SDS/PAGE method with gradient gels containing 8–16 % polyacrylamide. Before electrophoresis, samples were precipitated with trichloroacetic acid, washed twice with ice-cold acetone and dried [38].

Analysis of the functional mode of inactivation of PAI-1 by reaction with uPA and SDS/PAGE

Samples (5 μg) of PAI-1, which had been incubated as indicated for each single experiment, were mixed with 10 μg of uPA, at a PAI-1 concentration of 0.2 μM or 10 μg/ml, and a uPA concentration of 0.4 μM or 20 μg/ml. After incubation for 30 min, the samples were precipitated with trichloroacetic acid and subjected to SDS/PAGE (11 % gel). The gels were stained with Coomassie Blue. In this analysis, inhibitory active PAI-1 will be recovered as a complex with uPA with M_r approx. 100000. PAI-1 exhibiting substrate behaviour will be recovered as a large N-terminal fragment produced by reactive centre cleavage, whereas the only 33-amino-acid-long C-terminal fragment will not be recovered by the gel system used in the present study. Inert PAI-1, for instance the latent form, will be recovered in the position of native PAI-1.

Measurement of the specific inhibitory activity of PAI-1

The specific inhibitory activity of PAI-1, i.e. the fraction of the total amount of PAI-1 forming a stable complex with uPA under the conditions used, was measured by titration against uPA in a peptidyl anilide assay. Shortly, PAI-1 was diluted serially with HBS, supplemented with 0.25 % gelatin at 37 °C, corresponding to concentrations between 0.4 nM (20 ng/ml) and 400 nM (20 μg/ml) in a volume of 100 μl. Portions of uPA solutions maintained at the same temperature and the same buffer were then added, corresponding to a final uPA concentration of 5 nM (0.25 μg/ml), a final volume of 200 μl and final PAI-1 concentrations between 0.2 nM (10 ng/ml) and 200 nM (10 μg/ml). Incubation was then continued until the process of inhibition of uPA had come to an end (requiring < 2 min). The remaining uPA enzyme activity was determined by incubating with the peptidyl anilide substrate S-2444 at 37 °C and measuring A_{405}. The specific inhibitory activity of PAI-1, as percentage of the theoretical maximum, was calculated from the amount of PAI-1 that had to be added to inhibit 50 % of the 5 nM uPA.

To determine the IC_{50} values for the inactivation of PAI-1 by XR5118 or bis-ANS, individual dilution series of PAI-1 were incubated with a certain concentration of these compounds for 10 min before adding the uPA. The specific inhibitory activity was then determined as described above. The specific inhibitory activities were plotted against the concentration of the compound, and the IC_{50} values read as the concentrations halving the specific inhibitory activity.

Measurement of latency transition rate of PAI-1

PAI-1 (0.4 μM or 20 μg/ml) was incubated at 37 °C in HBS, supplemented with 0.25 % gelatin. At 1 h intervals, samples were withdrawn for measurement of specific inhibitory activity of PAI-1. The latency transition half-lives were calculated from semi-logarithmic plots of specific inhibitory activity versus time.

Limited proteolysis of PAI-1

PAI-1 (0.4 μM or 20 μg/ml in HBS), after preincubation with or without XR5118 as indicated for each single experiment, was digested with various proteases in a concentration of 1 μg/ml. For digestion with papain, the buffer was supplemented with 0.5 mM cysteine and 0.1 mM EDTA. For SDS/PAGE analysis, digestion was stopped by the addition of trichloroacetic acid to a final concentration of 7 % (w/v). For MS, digestion was stopped by 1 mM PMSF or 1 mM di-isopropylfluorophosphate.

N-terminal amino acid sequencing

N-terminal sequencing was performed on an Applied Biosystems model 477A gas-phase sequencer. In some cases, digested proteins were subjected to SDS/PAGE, transferred electrophoretically on to PVDF filters and sequenced from the filters. In other cases, the sequences were determined directly on trichloroacetic acid-precipitated digested protein.

MS

Samples were desalted on μC-18 ZipTips (Millipore Corp., Glostrup, Denmark), eluted with 4 mg/ml α-cyano-4-hydroxycinnamic acid in 50 % (w/v) acetonitrile, 0.1 % trifluoroacetic acid and applied directly to the matrix-assisted laser-desorption ionization–time-of-flight-MS target plate. Mass spectra were recorded in a Voyager DE PRO mass spectrometer (Applied Biosystems) operated in linear mode. Matrix-assisted laser-desorption ionization spectra were calibrated externally using corticotropin (ACTH; residues 18–39), apomyoglobin, bovine insulin and thioredoxin, giving mass determination accuracy better than 0.1 %. The assignment of different molecular species to individual peaks in the mass spectra was performed with the program GPMAW (Lighthouse Data, Odense, Denmark; http://welcome.to/gpmaw) and m/z (http://canada.proteometrics.com).

Vitronectin–PAI-1-binding assay

Vitronectin binding was compared for XR5118-treated latent or active PAI-1 (incubated at a concentration of 0.4 μM or 20 μg/ml in HBS for 20 min at 37 °C in the presence of 100 μM XR5118) and control active or latent PAI-1 (incubated at a concentration of 0.4 μM or 20 μg/ml in HBS for 20 min at 37 °C in the presence of XR5118 vehicle). The incubations were stopped by chilling on ice and a 2-fold dilution in PBS [10 mM Na_2HPO_4 (pH 7.4)/140 mM NaCl] with 2 % (w/v) milk, thus stopping further effects of XR5118.

For the binding assay, vitronectin was coated on to the solid phase of Maxisorb microtitre plates (Nunc A/S, Roskilde, Denmark), using 100 μl of 10 ng/ml vitronectin in 50 mM $NaHCO_3$ (pH 9.6) per well and incubation for 1 h at 4 °C. The wells were blocked using 2 % milk in PBS. Aliquots (100 μl) of control or XR5118-treated latent or active PAI-1 were added to the wells in concentrations between 10 μg/ml and 0.15 ng/ml, followed by 1 h incubation at ambient temperature (20 °C). The amount of PAI-1 bound to the solid phase was estimated with a layer of rabbit polyclonal anti-PAI-1 antibodies, a layer of peroxidase-conjugated swine anti-rabbit IgG and a peroxidase reaction. The signals obtained were corrected for the background signal in vitronectin-coated wells incubated with a vitronectin-binding-deficient PAI-1 variant (J. K. Jensen, unpublished work). The vitronectin affinity of XR5118-treated PAI-1 and latent PAI-1 relative to that of control PAI-1 were calculated as ratios of concentrations of the different forms giving the same signal in the assay.

Measurement of heat stability of PAI-1

Active or latent PAI-1 (2 μM or 100 μg/ml) in HBS was incubated for 30 min at 37 °C with 100 μM XR5118 or XR5118 vehicle. Aliquots of the differently treated portions of PAI-1 were then incubated at different temperatures between 0 and 100 °C for 2 h at the same concentration. In the temperature range between 50 and 70 °C, 5 °C intervals were used. After incubation, the samples were cooled on ice and centrifuged at 10000 ***g*** for 10 min. Aliquots (35 μl) from the supernatants were subjected to SDS/PAGE (11 % gel). The gels were stained with Coomassie Blue. Intensities of the bands were quantified using ImageQuant software and expressed relative to the intensity of the band corresponding to PAI-1 incubated at 0 °C. The temperature for precipitation of half of the PAI-1 was read from plots of relative solubility versus temperature.

Transverse urea gradient (TUG)/PAGE

Polyacrylamide running gels (7 %) were cast with a continuous gradient of urea from 0 to 8 M, using the buffer system also used for native-gel electrophoresis [26]. Electrophoresis was performed with 0.02 % Coomassie Blue in the cathode buffer [39]. Samples (30 μg) were applied in each gel run. Owing to a

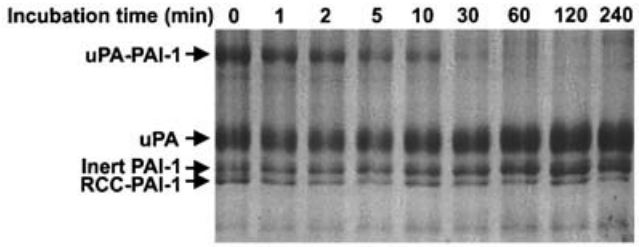

Figure 2 Functional assay of time course of XR5118 inactivation of PAI-1

PAI-1 (0.4 μM or 20 μg/ml) was incubated in HBS with 100 μM XR5118 at 37 °C. After incubation for the indicated time periods, samples corresponding to 5 μg of PAI-1 were incubated with 10 μg of uPA for 30 min at 37 °C and then subjected to SDS/PAGE. The positions of the uPA–PAI-1 complex, native/inert PAI-1, P_1–P_1'-cleaved PAI-1 (RCC-PAI-1) and uPA are indicated by arrowheads on the left.

slight irreproducibility in the casting of the gels, the shapes of protein bands were not reproducible completely from gel to gel. Comparison of the migration of two different PAI-1 forms was therefore done by electrophoresing mixtures of the two forms. Before mixing XR5118-treated PAI-1 and control PAI-1, the sample of XR5118-treated PAI-1 was passed through a layer of Sepharose [26] to remove excess XR5118 and avoid exposure of the added control PAI-1 to XR5118.

Statistical analysis

Results were analysed by Student's *t* test. Differences in results with a P value < 0.025 were considered statistically significant.

Structural analysis

Swiss PDB Viewer (http:/us.expasy.org/spdbv/) was used to display the three-dimensional structures of various PAI-1 forms.

RESULTS

Functional mode of inactivation of PAI-1 by XR5118

The effect of XR5118 on the functional behaviour of PAI-1 was analysed by reacting PAI-1, which had been exposed to XR5118 for different periods of time, with a molar excess of uPA and separating the reaction products by SDS/PAGE (Figure 2). Control experiments ensured that the reaction between PAI-1 and uPA was unaffected by XR5118 vehicle alone (results not shown). Without incubation with XR5118, most of the PAI-1 was in the active conformation and formed a stable, SDS-resistant complex with uPA, whereas a minor fraction was inert to uPA and was probably latent, and another minor fraction exhibited substrate behaviour. After the addition of XR5118, the amount of active PAI-1 capable of forming a complex with uPA disappeared and the amount of unmodified PAI-1 increased, indicating that XR5118 converts PAI-1 from the active form into an inert form. The rate of this activity loss is much larger than that of inactivation of PAI-1 caused by latency transition, occurring with a half-life of approx. 60 min (results not shown).

As shown in Figure 3, exposure of PAI-1 to Triton X-100 at 37 °C results in rapid conversion into a form with an increased tendency to substrate behaviour, followed by an accelerated conversion into the latent form [40]. When XR5118 is present in addition to Triton X-100, the remaining fraction of active PAI-1 is not only inactivated rapidly, but substrate behaviour is also quenched rapidly, in favour of an increased fraction of inert PAI-1 (Figure 3).

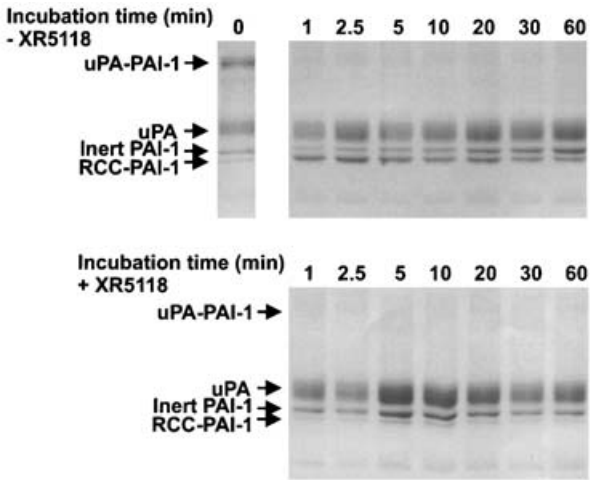

Figure 3 Inhibition by XR5118 of Triton X-100-induced substrate behaviour

PAI-1 (0.4 μM or 20 μg/ml) was incubated in HBS with 0.2 % Triton X-100 at 37 °C in the absence or presence of 100 μM XR5118. After incubation for the indicated time periods, samples corresponding to 5 μg of PAI-1 were incubated with 10 μg of uPA for 30 min at 37 °C and then subjected to SDS/PAGE. The positions of the uPA–PAI-1 complex, native/inert PAI-1, P_1–P_1'-cleaved PAI-1 (RCC-PAI-1) and uPA are indicated on the left.

Thus XR5118 inhibits the access of uPA to the RCL of PAI-1, both in native, active PAI-1 and in the Triton X-100-induced substrate form of PAI-1.

Proteolytic susceptibility of XR5118-neutralized PAI-1

In the absence of inactivators, a few specific peptide bonds in PAI-1 are susceptible to proteolysis by non-target proteases, localized mainly in the RCL and the flexible joint region [36,41–43]. In the present study, we investigated the effect of XR5118 on the susceptibility of PAI-1 to the non-target proteases elastase, endoprotease Glu-C, endoprotease Lys-C, papain and subtilisin. The cleavage sites were determined by a combination of N-terminal amino acid sequencing, MS, identification of N-terminal fragments with N-terminally ^{32}P-labelled PAI-1, SDS/PAGE and, in a few cases, digestion of PAI-1 mutated in protease-recognition sites. A representative analysis is shown in Figure 4 and a summary of the results obtained is given in Table 1. XR5118 vehicle alone did not affect the proteolytic susceptibility of PAI-1 (results not shown).

In control PAI-1, the main elastase cleavage site is the V345–S346 (P_4–P_3) bond [41]. XR5118 caused an inhibition of the elastase cleavability of the V345–S346 (P_4–P_3) bond and increased the accumulation of two additional cleavage products, which migrated in SDS/PAGE to positions corresponding to M_r approx. 28000 and 20000 respectively. Their N-termini were determined at R135 and Q206 respectively, showing that the major elastase-susceptible peptide bonds in XR5118-treated PAI-1 are the A134–R135 and the A205–Q206 bonds.

The main cleavage site for endoprotease Glu-C in control PAI-1 was previously found to be the E332–S333 bond, at the hinge between s5A and RCL [41]. The E332–S333 bond remained cleavable by endoprotease Glu-C in XR5118-treated PAI-1 (Figure 4). XR5118 induced endoprotease Glu-C cleavability of the E283–T284 and E285–V286 bonds. Other induced cleavage sites were minor.

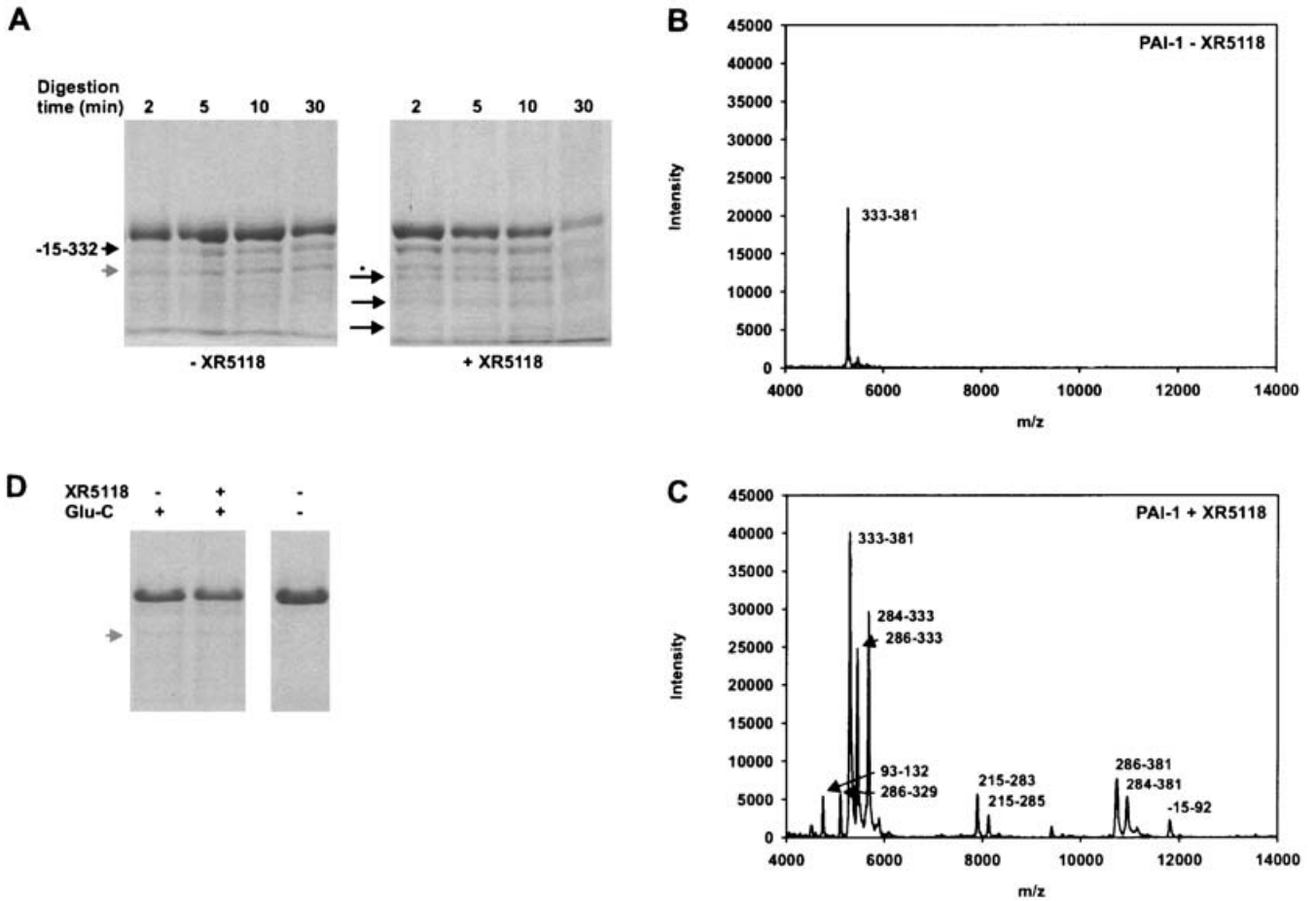

Figure 4 Proteolytic susceptibility of XR5118-neutralized PAI-1

Active or latent PAI-1 (0.4 μM or 20 μg/ml) were incubated with or without 100 μM XR5118 for 30 min at 37 °C, and subsequently digested at 37 °C with 3 μg/ml endoprotease Glu-C. (**A**) Control active or XR5118-inactivated PAI-1 was digested. The digestion was stopped with trichloroacetic acid at the indicated time points and the digests analysed by SDS/PAGE. The grey arrow indicates the position of endoprotease Glu-C. The large fragment consisting of amino acids −15 to 332, resulting from cleavage of the E332–S333 bond in both control active and XR5118-inactivated PAI-1, is indicated. Long black arrows indicate XR5118-induced fragments. The band indicated with an arrow and asterisk was identified as the fragments −15 to 283 and −15 to 285 by N-terminal ^{32}P-labelling and analysis of the mutants E283A and E285A. (**B**, **C**) Digestion of control active or XR5118-inactivated PAI-1 with endoprotease Glu-C was stopped with 1 mM PMSF after 2 min. The digests were analysed by MS. The minor digestion products indicated quantitatively minor cleavages at the E92–I93, E132–R133, E214–T215 and E329–V330 bonds. (**D**) Control or XR5118-treated latent PAI-1 was exposed to endoprotease Glu-C for 5 min and the digests analysed by SDS/PAGE. Latent PAI-1 was resistant to endoprotease Glu-C in the absence and presence of XR5118.

Table 1 Effect of XR5118 on the susceptibility of PAI-1 to non-target proteases

For brevity, the one-letter system for amino acids has been used, for example, S346 means Ser^{346}. n.d., not determined.

Protease	Cleavage sites (control PAI-1)	Secondary structural element	Cleavage sites (XR5118-treated PAI-1)	Secondary structural element
Elastase	V345–S346 (P_4–P_3) [42]	RCL	A134–S135 A205–Q206	hF s3C
Endoprotease Glu-C	E332–S333	s5A-RCL hinge	E332–S333 E283–T284 E285–V286	s5A-RCL hinge s6A s6A
Endoprotease Lys-C	Slow cleavage of K325A-V326	s5A	Fast cleavage of K325A-V326	s5A
Papain	S346-V347 (P_3–P_2) [42]	RCL	n.d., but cleavage in RCL reduced	
Subtilisin	V345-S346 (P_4–P_3) [43] A347-R348 (P_2–P_1) [43] R348-M349 (P_1–P_1') [43]	RCL RCL RCL	n.d., but cleavage in RCL reduced	

XR5118 treatment strongly increased endoprotease Lys-C cleavability of the K325–V326 bond. No other major endoprotease Lys-C cleavage sites were detected.

In control PAI-1, the main cleavage sites for papain and subtilisin are in the RCL. The cleavage site for papain is the S346–A347 (P_3–P_2) bond [41] and those for subtilisin are the V345–S346 (P_4–P_3) bond, the A347–R348 (P_2–P_1) bond and the R348–M349 (P_1–P_1') bond [43]. SDS/PAGE analysis showed that the corresponding fragments did not accumulate with XR5118-treated PAI-1. XR5118-treated PAI-1 had a generally increased rate of proteolysis by papain and subtilisin, but we were not able to distinguish major, primary cleavage sites from secondary ones outside the RCL.

On this basis, we concluded that the RCL of XR5118-treated PAI-1 is protected against non-target proteases, but that other parts of the molecule display a strongly increased susceptibility to non-target proteases.

The digestion pattern for XR5118-treated PAI-1 described above is clearly different from that previously reported for latent PAI-1 [36,41,43]. Control experiments ensured that treatment of latent PAI-1 with XR5118 did not change the digestion pattern (Figure 4 and results not shown). We therefore concluded that the XR5118-induced form of PAI-1 is different from the latent form.

Characterization of the stability of XR5118-inactivated PAI-1

The urea-unfolding pattern of XR5118-treated PAI-1 was studied by TUG/PAGE. Although latent and P_1–P_1' bond-cleaved PAI-1 had a urea-unfolding pattern clearly different from that of active PAI-1, we observed no difference between active and XR5118-inactivated PAI-1 (Figure 5).

The temperatures resulting in the precipitation of half of control active PAI-1 and XR5118-inactivated PAI-1 were determined to be 47 $\pm$ 2 °C ($n = 3$) and 55 $\pm$ 3 °C ($n = 3$) respectively. The temperatures resulting in the precipitation of half of the control latent PAI-1 and XR5118-treated latent PAI-1 were determined to be 55 $\pm$ 5 °C ($n = 3$) and 58 $\pm$ 5 °C ($n = 3$) respectively. Thus the temperatures for the precipitation of half of the XR5118-inactivated PAI-1, control latent PAI-1 and XR5118-treated latent PAI-1 were indistinguishable, but significantly different from that of control active PAI-1 ($P < 0.025$). There was no measurable precipitation of P_1–P_1'-cleaved PAI-1 at temperatures below 75 °C.

Effect of XR5118 on the binding of PAI-1 to vitronectin

Measuring the binding of control active and XR5118-inactivated PAI-1 to vitronectin immobilized on the solid phase, we found that XR5118 inactivation was associated with a considerable decrease in the affinity to vitronectin. The affinity of latent PAI-1 to vitronectin remained much lower than that of active PAI-1, irrespective of whether latent PAI-1 had been exposed to XR5118 or not (Figure 6). XR5118-inactivated PAI-1 remained inactive after 1 h incubation at ambient temperature with vitronectin (results not shown).

Effect of alanine substitutions on the susceptibility of PAI-1 to XR5118

Alanine-scanning mutagenesis was performed, both to locate the XR5118-binding site and to study the spread of XR5118-induced conformational changes. We measured the IC_{50} values for XR5118 inactivation of a number of variants, using a 10 min preincubation with various XR5118 concentrations before measuring the specific inhibitory activities (Table 2). The IC_{50} value for XR5118 inactivation of wild-type (wt) PAI-1 was 12 μM. Most mutants did not differ from wt PAI-1 with respect to susceptibility to XR5118. Some mutants, including T96A, Q102A, S121A, F136A, E285A and K325A, were totally inhibited by XR5118 at sufficiently high concentrations, but had an increased IC_{50} value. Other mutants,

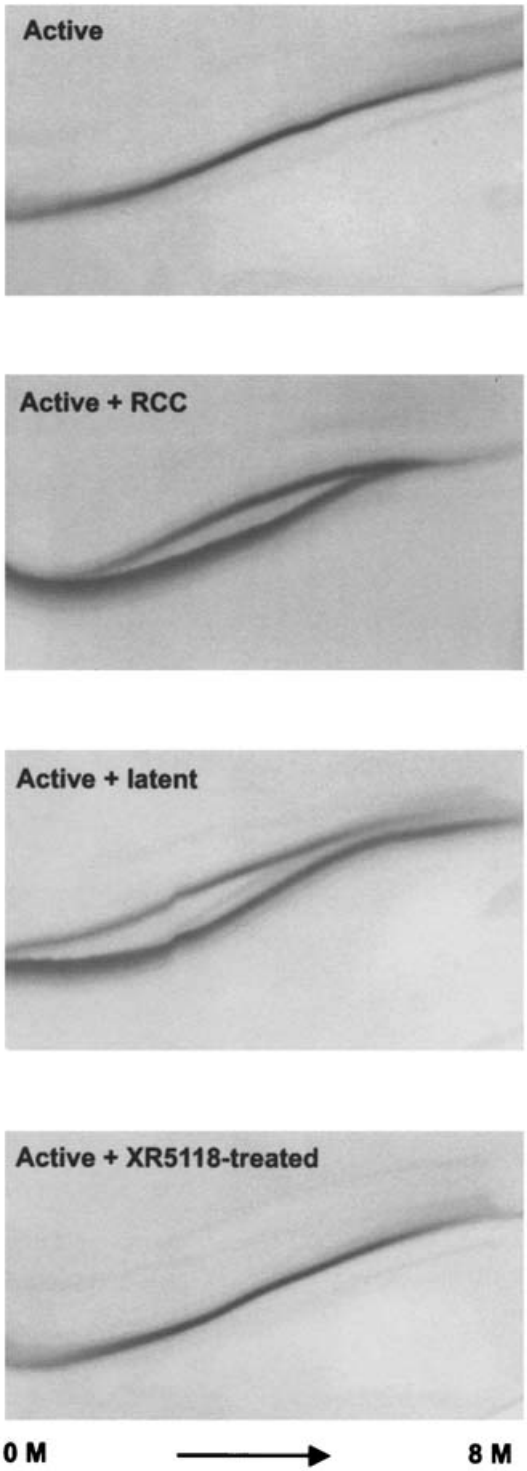

Figure 5 Effect of XR5118 on PAI-1 as analysed by TUG/PAGE

The indicated PAI-1 forms were electrophoresed in polyacrylamide gels with a reverse 0–8 M urea gradient. RCC, P_1–P_1'-cleaved PAI-1.

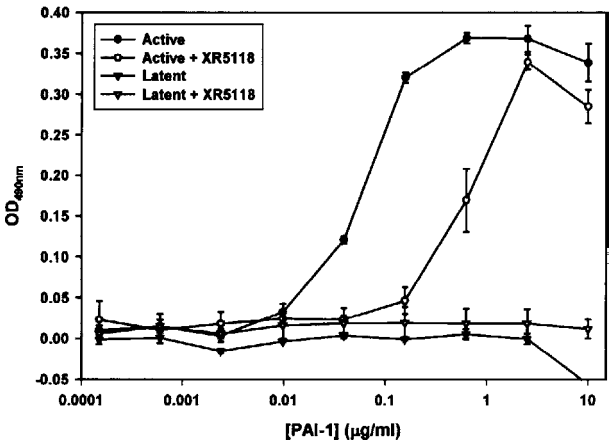

Figure 6 Effect of XR5118 on PAI-1–vitronectin binding

The indicated concentrations of the indicated forms of PAI-1 were incubated in wells of vitronectin-coated microtitre plates. The *y*-axis shows A_{490}, after correction for the readings in vitronectin-coated plates incubated with a vitronectin-binding-deficient PAI-1 variant. The symbols indicate the means and S.D. for triple determinations.

Table 2 Effect of amino acid substitutions on the susceptibility of PAI-1 to XR5118

IC_{50} values are means ± S.D., and the number of determinations are in parentheses. The following mutants were also tested, but found to be indistinguishable from wt with respect to the susceptibility to XR5118: S37A, Y39A, E55A, Q57A, Q59A, Q61A, K67A, L77A, R78A, Y81A, R103A, D104A, K106A, L107A, Q109A, M112A, P113A, F116A, R117A, F119A, R120A, T122A, K124A, Q125A, S129A, E130A, V131A, E132A, R133A, R135A, I138A, D140A, V142A, K143A, T144A, H145A, K147A, M149A, N152A, D160A, R164A, N169A, E283A, D299A, R302A, F304A, Q305A, D307A, T309A, D313A, E315A, P316A, Q321A and K327A. D127A could not be analysed due to low yield in the expression system and almost complete lack of activity. The IC_{50} values for all of the mutants shown in the table were significantly different from wt ($P < 0.01$). *V126A and I137A displayed a heterogeneous response to XR5118: 54 ± 7% ($n = 5$) and 57 ± 19% ($n = 10$) of the total inhibitory activity, respectively, were totally inhibited by 5 μM XR5118, whereas the rest of the activity was totally resistant to XR5118 concentrations up to 250 μM. For further explanation, see the text.

Mutant	IC_{50} (μM)	Secondary structural element
wt	12 ± 5 (53)	
T96A	45 ± 22 (5)	s2A
F100A	> 250 (3)	s2A
Q102A	56 ± 15 (5)	s2A
S121A	35 ± 9 (5)	s1A
V126A	< 5 and > 250 (5)*	s1A
F128A	> 250 (3)	s1A/hF loop
F136A	35 ± 15 (9)	hF
I137A	< 5 and > 250 (10)*	hF
N139A	> 250 (3)	hF
W141A	> 250 (3)	hF
T146A	> 250 (3)	hF
E285A	33 ± 13 (3)	s6A
K325A	38 ± 15 (8)	s5A
N152H-K156T-Q321L-M356I	> 250 (3)	hF/s3A loop, s5A and s1C

including F100A, F128A, N139A, W141A, T146A and the so-called 'stable' PAI-1 N152H-K156T-Q321L-M356I [44], had an IC_{50} value higher than 250 μM, approaching the highest XR5118 concentration soluble in water. The two mutants V126A and I137A displayed a heterogeneous response to XR5118, about half of their total inhibitory activity being totally inhibited by 5 μM XR5118, whereas the rest of the activity was totally resistant to XR5118 concentrations up to 250 μM, probably reflecting folding of a fraction of these variants into an unstable form.

A functional characterization of these mutants in the absence of XR5118 showed that the half-lives of the specific inhibitory activity, i.e. the half-lives for latency transition of T96A, F100A, Q102A, S121A, V126A, F128A and F136A are between 0.5- and 1.4-fold the half-life of wt, that of K325A is 1.7-fold that of wt and those of I137A, N139A, W141A and T146A are more than 3-fold that of wt [45]. 'Stable' PAI-1 N152H-K156T-Q321L-M356I has a latency transition half-life of approx. 60 h [44]. The specific inhibitory activities of T96A, Q102A, S121A, F136A, E285A and K325A were found to be normal. However, F100A, V126A, F128A, I137A, N139A, W141A and T146A have low specific inhibitory activities, of the order of magnitude of 10% of wt, correlated with a high fraction being in a stable substrate form, with the half-life for conversion of the substrate form into the latent form being more than 15 h [45]. The substrate forms of these mutants were also resistant to XR5118 in the sense that XR5118 did not affect their uPA-catalysed substrate cleavage, i.e. with these mutants, the amount of cleaved PAI-1 did not change during incubation with XR5118, neither did this substrate form convert into the XR5118-induced inert form seen with PAI-1 wt (results not shown). The mutation-induced substrate forms thereby differ from the Triton X-100-induced substrate form of PAI-1 wt, which is not cleaved in the presence of XR5118 (Figure 3).

For comparison, the above-mentioned mutants were also tested with respect to bis-ANS inactivation of the PAI-1-inhibitory activity. Among these, only N152H-K156T-Q321L-M356I (stable PAI-1) had a changed IC_{50} value for bis-ANS inactivation of PAI-1 (results not shown).

DISCUSSION

XR5118 induces an inert monomeric form of PAI-1, clearly different from the polymeric form induced by negatively charged inactivators like bis-ANS [26]. Measurements of the proteolytic susceptibility of control and XR5118-inactivated PAI-1 showed that XR5118 rendered the RCL less susceptible to non-target proteases. This observation is in good agreement with XR5118-inactivated PAI-1 being inert to uPA (Figure 2) and with XR5118 even inhibiting Triton-X-100-induced substrate behaviour (Figure 3), showing that XR5118 decreases the accessibility of the RCL to the target protease uPA. On the other hand, XR5118 induced increased proteolytic susceptibility of peptide bonds elsewhere in PAI-1, suggesting a generally increased flexibility. Interestingly, a proteolytic hot spot seemed to be induced in the central areas of s5A and s6A (Table 1 and Figure 7). The proteolytic susceptibility of XR5118-inactivated PAI-1 was different from that of the latent form and XR5118 treatment did not change the migration of PAI-1 in TUG/PAGE (Figure 5). We therefore concluded that XR5118-inactivated PAI-1 is different from latent PAI-1. In addition, TUG/PAGE (Figure 5) and measurements of heat stability showed that XR5118-inactivated PAI-1 is clearly different from P_1–P_1'-cleaved PAI-1. But XR5118 treatment did result in an increase in heat stability similar to that observed on latency transition and in a slight decrease in affinity to vitronectin (Figure 6).

We found that specific alanine residue substitutions decreased the susceptibility of PAI-1 to XR5118. The susceptibility of a PAI-1 mutant to an inactivator depends both on the binding affinity of the inactivator and on the rate of inactivator-induced conformational change. Besides the changed susceptibility to XR5118, some of the mutants also had other changes in functional properties. Latency transition rates of XR5118-resistant mutants I137A, N139A, W141A and T146A are more than 3-fold longer

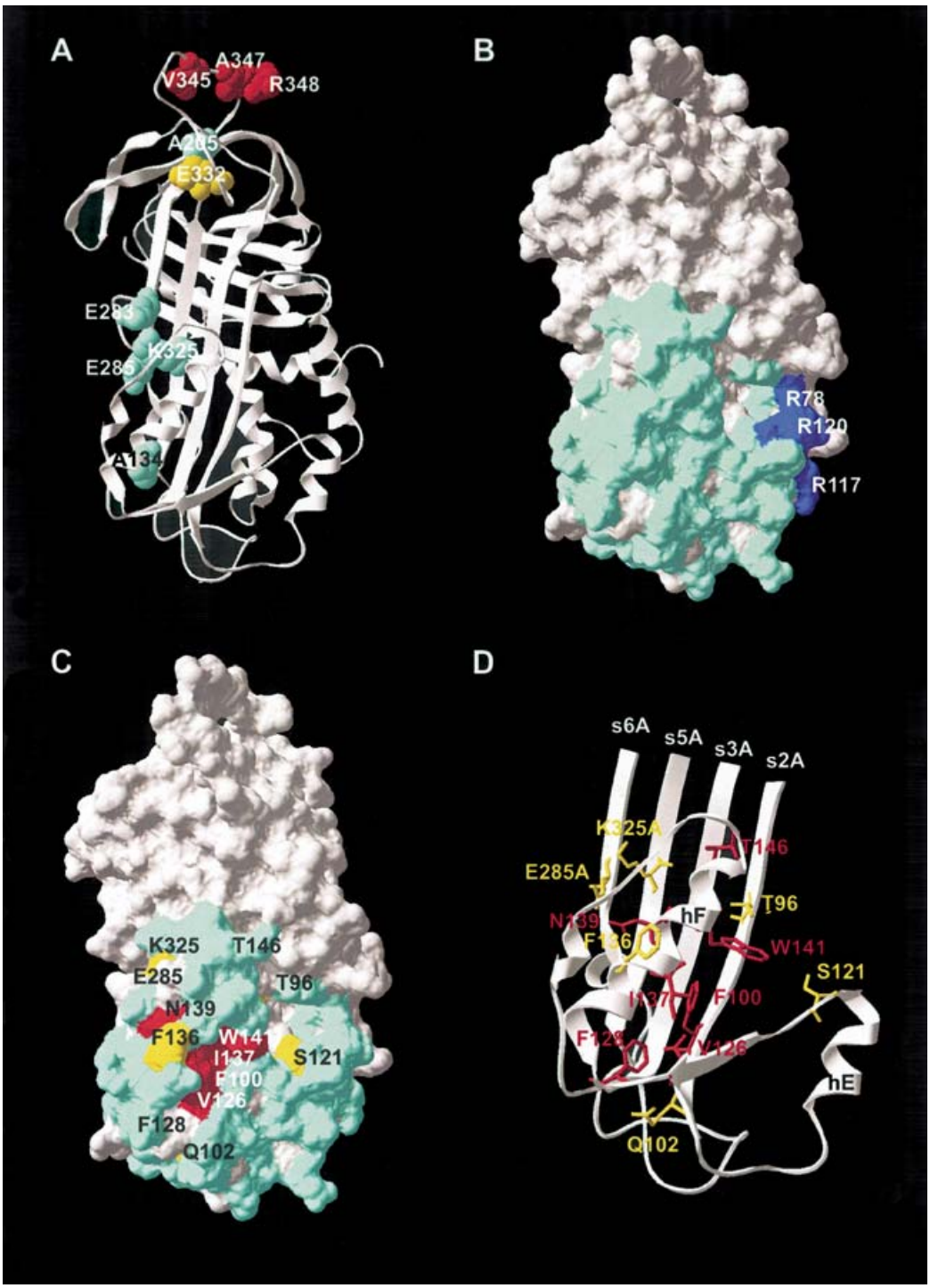

Figure 7 Proteolytic cleavage sites and neutralizer effector sites displayed on the three-dimensional structure of PAI-1

(**A**) Proteolytic cleavage sites, shown on a ribbon presentation of the PAI-1 structure. Residues C-terminal to proteolytic cleavage sites are indicated in spacefill. Cyan residues indicate peptide bonds with increased susceptibility in XR5118-inactivated PAI-1. Red residues indicate peptide bonds with decreased proteolytic susceptibility in XR5118-inactivated PAI-1. The yellow residue indicates the peptide bond with unchanged proteolytic susceptibility in XR5118-inactivated PAI-1. (**B**) Effector sites for bis-ANS, shown on a surface presentation of the PAI-1 structure. Substitution of the cyan residues did not result in changes of the IC_{50} value for bis-ANS inactivation of PAI-1. The dark blue residues are those involved previously [26] in bis-ANS inactivation of PAI-1 by charge-reversal mutations. Note that D299, R302, F304, Q305, D307, T309, D313, E315 and P316, all found to be not important for the bis-ANS response, are not visible, as they are localized on the back of the structure. (**C**) Effector sites for XR5118, displayed on a surface presentation of the PAI-1 structure. Substitution of the red residues resulted in an IC_{50} value above 250 μM for XR5118 inactivation of PAI-1. Substitution of the yellow residues resulted in an IC_{50} value below 250 μM for XR5118 inactivation of PAI-1, but significantly different from the IC_{50} value for PAI-1 wt. Substitution of the cyan residues did not result in changes of the IC_{50} value for XR5118 inactivation of PAI-1. A and G residues in the 90–170 sequence are also shown in cyan. T96, Q102, F128 and T146 are not or only partly visible. Note that D299, R302, F304, Q305, D307, T309, D313, E315 and P316, all found to be not important for the XR5118 response, are not visible, as they are localized on the back of the structure. (**D**) Effector sites for XR5118, displayed on a ribbon and wireframe presentation of a part of the structure. Substitution of the red residues resulted in an IC_{50} value above 250 μM for XR5118 inactivation of PAI-1. Substitution of the yellow residues resulted in an IC_{50} value below 250 μM for XR5118 inactivation of PAI-1, but significantly different from the IC_{50} value for PAI-1 wt. All structures are in the same orientation. The Figures are Swiss-PDB-Viewer displays of the X-ray crystal structure as determined by Sharp et al. [24].

than that of wt. Moreover, a large fraction of these mutants and the likewise XR5118-resistant mutants F100A, V126A and F128A are folded into stable substrate forms [45], which are resistant to XR5118 in the sense that they maintain substrate behaviour in the presence of XR5118 (results not shown), thereby differing from the Triton X-100-induced substrate form (Figure 3). The residues substituted in these mutants are localized at the interface between hF and β-sheet A (F100A, V126A, F128A, I137A and W141A) or localized in hF and within hydrogen-bonding distance of the loop connecting hF and s3A, namely the hF–s3A loop (N139A and T146A; Figure 7). We believe that the stability of the substrate forms of F100A, V126A, F128A, I137A, N139A, W141A and T146A and the decreased latency transition rate of I137A, N139A, W141A and T146A are caused by a decreased mobility of hF and the hF–s3A loop and a concomitant decreased rate of RCL insertion [45]. A fundamental role for the stability of Y160 of α_1-anti-trypsin, corresponding to W141 of PAI-1, was demonstrated recently [46]. We therefore propose that a decreased hF and hF–s3A loop mobility also prevents the XR5118-induced conformational change and thereby increases the IC_{50} value for these variants. This interpretation is supported by the observation of XR5118 resistance of the 'stable' PAI-1 mutant N152H-K156T-Q321L-M356I, as the stabilization of this variant seemed to depend on a change in the configuration of the hF–s3A loop and its interactions with hF and β-sheet A, restricting the mobility of hF and the hF–s3A loop relative to the remainder of the molecule [24,25]. Likewise, alanine substitutions for E285 or K325 also decreased the susceptibility to XR5118. Being localized in close proximity in s6A and s5A respectively, the side chains of both residues point towards the hF–s3A loop (Figure 7). K325 has been previously suggested to play a role in communication between the RCL and the flexible joint region, and hF [34,47–49]. We propose that E285 and K325 participate in conveying the XR5118-induced conformational change from hF to the RCL. Involvement of the central parts of s5A and s6A in the XR5118 effect is further supported by proteolytic digestion analysis (see above).

On the other hand, other mutants with substitutions at the hF–β-sheet A interface (T96A, Q102A, S121A and F136A) had changed IC_{50} values for XR5118 inactivation without consistent substantial changes in specific inhibitory activities and latency transition half-lives. This observation would be in agreement with XR5118 binding between hF and s2A on the one side and s1A on the other. The hypothesis that XR5118 binds in this region is also in agreement with the previously reported observations that XR5118 and the negatively charged inactivators compete for binding to PAI-1 [26], and that mutations in the flexible joint region decrease the effect of negatively charged inactivators (Figure 7 and [26,29]). This proposal is also in accordance with a previous observation of a 50% decrease in the binding of XR5118-treated PAI-1 by an antibody with epitope in the 112–147 sequence [28]. Remarkably, however, mutations decreasing the susceptibility to XR5118 and those decreasing the susceptibility to bis-ANS are different (Figure 7 and [26]). Therefore it appears that the differential effects of the two groups of inactivators are associated with non-identical, although overlapping, binding sites.

We recently presented evidence that the vitronectin-binding site is constituted mainly of residues in the s2A–hE loop, hE and s1A, but may also involve F100, I137A, D140A and W141 [34] and, thus, may partly overlap with the proposed XR5118-binding site. Accordingly, XR5118 inactivation was associated with a significant decrease in vitronectin affinity. It was clear that XR5118-inactivated PAI-1 cannot be reactivated by vitronectin, although vitronectin, when added before XR5118, does protect against the inactivation [26,49]. This observation is in line with the previous finding that XR5118-inactivated PAI-1 remains inactive after the removal of free and reversibly bound XR5118 by BSA [26].

In summary, our results are consistent with a hypothesis that XR5118 binds in an area between s1A on the one side and hF and s2A on the other, where it may make contact with T96, Q102, S121, F136 and also F100, V126, F128, I137 and W141, thereby changing the position of hF, initiating a conformational change spreading through the entire molecule, causing a generally increased flexibility, distortion of the centre of β-sheet A and changing the configuration and position of the RCL, making it inaccessible to the target proteases.

The excellent technical assistance of Tanja Christiansen is gratefully acknowledged. The work was supported by grants from the Danish Cancer Society, the Danish Natural Science Research Council, the Danish Research Agency, the Danish Cancer Research Foundation and the Novo-Nordisk Foundation.

REFERENCES

1 Andreasen, P. A., Egelund, R. and Petersen, H. H. (2000) The plasminogen activation system in tumor growth, invasion, and metastasis. Cell. Mol. Life Sci. **57**, 25–40
2 Booth, N. A. (1999) Fibrinolysis and thrombosis. Baillieres Best Pract. Res. Clin. Haematol. **12**, 423–433
3 Erickson, L. A., Fici, G. J., Lund, J. E., Boyle, T. P., Polites, H. G. and Marotti, K. R. (1990) Development of venous occlusions in mice transgenic for the plasminogen activator inhibitor-1 gene. Nature (London) **346**, 74–76
4 Eren, M., Painter, C. A., Atkinson, J. B., Declerck, P. J. and Vaughan, D. E. (2002) Age-dependent spontaneous coronary arterial thrombosis in transgenic mice that express a stable form of human plasminogen activator inhibitor-1. Circulation **106**, 491–496
5 Huber, K., Christ, G., Wojta, J. and Gulba, D. (2001) Plasminogen activator inhibitor type-1 in cardiovascular disease. Status report 2001. Thromb. Res. **103** (Suppl. 1), 7–19
6 Andreasen, P. A., Kjøller, L., Christensen, L. and Duffy, M. J. (1997) The urokinase-type plasminogen activator system in cancer metastasis. A review. Int. J. Cancer **72**, 1–22
7 Bajou, K., Noël, A., Gerard, R. D., Masson, V., Brünner, N., Holst-Hansen, C., Skobe, M., Fusenig, N. E., Carmeliet, P., Collen, D. et al. (1998) Absence of host plasminogen activator inhibitor 1 prevents cancer invasion and vascularization. Nat. Med. **4**, 923–928
8 Bajou, K., Masson, V., Gerard, R. D., Schmitt, P. M., Albert, V., Praus, M., Lund, L. R., Frandsen, T. L., Brünner, N., Danø, K. et al. (2001) The plasminogen activator inhibitor PAI-1 controls *in vivo* tumor vascularization by interaction with proteases, not vitronectin. Implications for antiangiogenic strategies. J. Cell Biol. **152**, 777–784
9 Lambert, V., Munaut, C., Noel, A., Frankenne, F., Bajou, K., Gerard, R., Carmeliet, P., Defresne, M. P., Foidart, J. M. and Rakic, J. M. (2001) Influence of plasminogen activator inhibitor type 1 on choroidal neovascularization. FASEB J. **15**, 1021–1027
10 McMahon, G. A., Petitclerc, E., Stefansson, S., Smith, E., Wong, M. K., Westrick, R. J., Ginsburg, D., Brooks, P. C. and Lawrence, D. A. (2001) Plasminogen activator inhibitor-1 regulates tumor growth and angiogenesis. J. Biol. Chem. **276**, 33964–33968
11 Devy, L., Blacher, S., Grignet-Debrus, C., Bajou, K., Masson, V., Gerard, R. D., Gils, A., Carmeliet, G., Carmeliet, P., Declerck, P. J. et al. (2002) The pro- or antiangiogenic effect of plasminogen activator inhibitor 1 is dose dependent. FASEB J. **16**, 147–154
12 Irving, J. A., Pike, R. N., Lesk, A. M. and Whisstock, J. C. (2000) Phylogeny of the serpin superfamily: implications of patterns of amino acid conservation for structure and function. Genome Res. **10**, 1845–1864
13 Wind, T., Hansen, M., Jensen, J. K. and Andreasen, P. A. (2002) The molecular basis for anti-proteolytic and non-proteolytic functions of plasminogen activator inhibitor-1: roles of the reactive centre loop, the shutter region, the flexible joint region, and the small serpin fragment. Biol. Chem. **283**, 21–36
14 Shore, J. D., Day, D. E., Francis-Chmura, A. M., Verhamme, I. M., Kvassman, J., Lawrence, D. A. and Ginsburg, D. (1995) A fluorescent probe study of plasminogen activator inhibitor-1. Evidence for reactive center loop insertion and its role in the inhibitory mechanism. J. Biol. Chem. **270**, 5395–5398
15 Lawrence, D. A., Ginsburg, D., Day, D. E., Berkenpas, M. B., Verhamme, I. M., Kvassman, J. O. and Shore, J. D. (1995) Serpin–protease complexes are trapped as stable acyl-enzyme intermediates. J. Biol. Chem. **270**, 25309–25312
16 Wilczynska, M., Fa, M., Ohlsson, P. I. and Ny, T. (1995) The inhibition mechanism of serpins. Evidence that the mobile reactive center loop is cleaved in the native protease-inhibitor complex. J. Biol. Chem. **270**, 29652–29655
17 Egelund, R., Rodenburg, K. W., Andreasen, P. A., Rasmussen, M. S., Guldberg, R. E. and Petersen, T. E. (1998) An ester bond linking a fragment of a serine protease to its serpin inhibitor. Biochemistry **37**, 6375–6379

18 Stratikos, E. and Gettins, P. G. (1999) Formation of the covalent serpin–protease complex involves translocation of the protease by more than 70 Å and full insertion of the reactive center loop into β-sheet A. Proc. Natl. Acad. Sci. U.S.A. **96**, 4808–4813
19 Fa, M., Bergström, F., Hägglöf, P., Wilczynska, M., Johansson, L. B.-Å. and Ny, T. (2000) The structure of a serpin–protease complex revealed by intramolecular distance measurements using donor–donor energy migration and mapping of interaction sites. Structure **8**, 397–405
20 Huntington, J. A., Read, R. J. and Carrell, R. W. (2000) Structure of a serpin–protease complex shows inhibition by deformation. Nature (London) **407**, 923–926
21 Egelund, R., Petersen, T. E. and Andreasen, P. A. (2001) A serpin-induced extensive proteolytic susceptibility of urokinase-type plasminogen activator implicates distortion of the protease substrate binding pocket and oxyanion hole in the serpin inhibitory mechanism. Eur. J. Biochem. **268**, 673–685
22 Ye, S., Cech, A. L., Belmares, R., Bergstrom, R. C., Tong, Y., Corey, D. R., Kanost, M. R. and Goldsmith, E. J. (2001) The structure of a Michaelis serpin–protease complex. Nat. Struct. Biol. **8**, 979–883
23 Mottonen, J., Strand, A., Symersky, J., Sweet, R. M., Danley, D. E., Geoghegan, K. F., Gerard, R. D. and Goldsmith, E. J. (1992) Structural basis of latency in plasminogen activator inhibitor-1. Nature (London) **355**, 270–273
24 Sharp, A. M., Stein, P. E., Pannu, N. S., Carrell, R. W., Berkenpas, M. B., Ginsburg, D., Lawrence, D. A. and Read, R. J. (1999) The active conformation of plasminogen activator inhibitor 1, a target for drugs to control fibrinolysis and cell adhesion. Structure **7**, 111–118
25 Nar, H., Bauer, M., Stassen, J. M., Lang, D., Gils, A. and Declerck, P. J. (2000) Plasminogen activator inhibitor 1. Structure of the native serpin, comparison to its other conformers and implications for serpin inactivation. J. Mol. Biol. **297**, 683–695
26 Egelund, R., Einholm, A. P., Pedersen, K. E., Nielsen, R. W., Christensen, A., Deinum, J. and Andreasen, P. A. (2001) A regulatory hydrophobic area in the flexible joint region of plasminogen activator inhibitor-1, defined with fluorescent activity-neutralizing ligands. Ligand-induced serpin polymerization. J. Biol. Chem. **276**, 13077–13086
27 Charlton, P. A., Faint, R. W., Bent, F., Bryans, J., Chicarelli-Robinson, I., Mackie, I., Machin, S. and Bevan, P. (1996) Evaluation of a low molecular weight modulator of human plasminogen activator inhibitor-1 activity. Thromb. Haemost. **75**, 808–815
28 Friederich, P. W., Levi, M., Biemond, B. J., Charlton, P., Templeton, D., van Zonneveld, A. J., Bevan, P., Pannekoek, H. and ten Cate, J. W. (1997) Novel low-molecular-weight inhibitor of PAI-1 (XR5118) promotes endogenous fibrinolysis and reduces post thrombolysis thrombus growth in rabbits. Circulation **96**, 916–921
29 Björquist, P., Ehnebom, J., Inghardt, T., Hansson, L., Lindberg, M., Linschoten, M., Stromqvist, M. and Deinum, J. (1998) Identification of the binding site for a low-molecular-weight inhibitor of plasminogen activator inhibitor type 1 by site-directed mutagenesis. Biochemistry **37**, 1227–1234
30 Neve, J., Leone, P. A., Carroll, A. R., Moni, R. W., Paczkowski, N. J., Pierens, G., Björquist, P., Deinum, J., Ehnebom, J. and Inghardt, T. (1999) Sideroxylonal C, a new inhibitor of human plasminogen activator inhibitor type-1, from the flowers of *Eucalyptus albens*. J. Nat. Prod. **62**, 324–326
31 Gils, A., Stassen, J.-M., Nar, H., Kley, J. T., Wienen, W., Ries, U. J. and Declerck, P. J. (2002) Characterization and comparative evaluation of a novel PAI-1 inhibitor. Thromb. Haemost. **88**, 137–143
32 Christensen, J. H., Hansen, P. K., Lillelund, O. and Thøgersen, H. C. (1991) Sequence-specific binding of the N-terminal three-finger fragment of *Xenopus* transcription factor IIIA to the internal control region of a 5 S RNA gene. FEBS Lett. **281**, 181–184
33 Gill, S. C. and von Hippel, P. H. (1989) Calculation of protein extinction coefficients from amino acid sequence data. Anal. Biochem. **182**, 319–326
34 Jensen, J. K., Wind, T. and Andreasen, P. A. (2002) The vitronectin binding area of plasminogen activator inhibitor-1, mapped by mutagenesis and protection against an inactivating organochemical ligand. FEBS Lett. **521**, 91–94
35 Wind, T., Jensen, M. A. and Andreasen, P. A. (2001) Epitope mapping for four monoclonal antibodies against human plasminogen activator inhibitor type-1. Implications for antibody-mediated PAI-1 neutralisation and vitronectin binding. Eur. J. Biochem. **268**, 1095–1106
36 Egelund, R., Schousboe, S. L., Sottrup-Jensen, L., Rodenburg, K. W. and Andreasen, P. A. (1997) Type-1 plasminogen activator inhibitor. Conformational differences between latent, active, reactive-center-cleaved and plasminogen-activator-complexed forms, as probed by proteolytic susceptibility. Eur. J. Biochem. **248**, 775–785
37 Andreasen, P. A., Riccio, A., Welinder, K. G., Douglas, R., Sartorio, R., Nielsen, L. S., Oppenheimer, C., Blasi, F. and Danø, K. (1986) Plasminogen activator inhibitor type 1: reactive center and amino-terminal heterogeneity, determined by protein and cDNA sequencing. FEBS Lett. **209**, 213–218
38 Lovrien, R. and Matulis, D. (1995) Assays for total protein. In Current Protocols in Protein Science (Coligan, J. E., Dunn, B. M., Ploegh, H. L., Speicher, D. W. and Wingfield, P. T., eds.), John Wiley and Sons, New York
39 Schägger, H. and von Jagow, G. (1991) Blue native electrophoresis for isolation of membrane protein complexes in enzymatically active form. Anal. Biochem. **199**, 223–231
40 Gils, A. and Declerck, P. J. (1998) Modulation of plasminogen activator inhibitor 1 by Triton X-100 – identification of two consecutive conformational transitions. Thromb. Haemost. **80**, 286–291
41 Kjøller, L., Martensen, P. M., Sottrup-Jensen, L., Justesen, J., Rodenburg, K. W. and Andreasen, P. A. (1996) Conformational changes of the reactive-centre loop and β-strand 5A accompany temperature-dependent inhibitor–substrate transition of plasminogen-activator inhibitor 1. Eur. J. Biochem. **241**, 38–46
42 Andreasen, P. A., Egelund, R., Jensen, S. and Rodenburg, K. W. (1999) Solvent effects on activity and conformation of plasminogen activator inhibitor-1. Thromb. Haemost. **81**, 407–414
43 Zhou, A., Faint, R., Charlton, P., Dafforn, T. R., Carrell, R. W. and Lomas, D. A. (2001) Polymerization of plasminogen activator inhibitor-1. J. Biol. Chem. **276**, 9115–9122
44 Berkenpas, M. B., Lawrence, D. A. and Ginsburg, D. (1995) Molecular evolution of plasminogen activator inhibitor-1 functional stability. EMBO J. **14**, 2969–2977
45 Wind, T., Jensen, J. K., Dupont, D. M. and Andreasen, P. A. (2003) Mutational analysis of plasminogen activator inhibitor-1. Eur. J. Biochem. **270**, 1680–1688
46 Cabrita, L. D., Whisstock, J. C. and Bottomley, S. P. (2002) Probing the role of the F-helix in serpin stability through a single tryptophan substitution. Biochemistry **41**, 4575–4581
47 Schousboe, S. L., Egelund, R., Kirkegaard, T., Preissner, K. T., Rodenburg, K. W. and Andreasen, P. A. (2000) Vitronectin and substitution of a β-strand 5A lysine residue potentiate activity-neutralization of PA inhibitor-1 by monoclonal antibodies against α-helix F. Thromb. Haemost. **83**, 742–751
48 Hansen, M., Busse, M. N. and Andreasen, P. A. (2001) Importance of the amino-acid composition of the shutter region of plasminogen activator inhibitor-1 for its transitions to latent and substrate forms. Eur. J. Biochem. **268**, 6274–6283
49 Jensen, S., Kirkegaard, T., Pedersen, K. E., Busse, M., Preissner, K. T., Rodenburg, K. W. and Andreasen, P. A. (2002) The role of β-strand 5A residues of plasminogen activator inhibitor-1 in regulation of its latency transition and inhibitory activity by vitronectin. Biochim. Biophys. Acta **1597**, 301–310

Received 4 December 2002/27 March 2003; accepted 30 April 2003
Published as BJ Immediate Publication 30 April 2003, DOI 10.1042/BJ20021880